T 1017

EFFECT of STRAIN RATE on FLOW STRESS of COPPER

By

Raymond L. Straw

T 1017

A thesis submitted to the Faculty and the Board of Trustees of the Colorado School of Mines in partial fulfillment of the requirements for the degree of Master of Science in Metallurgical Engineering.

Signed: Raymond L. Straw
Raymond L. Straw

Golden, Colorado

Date: October 11 1965

Approved: J. D. Lubahn
J. D. Lubahn
Thesis Advisor

A. W. Schlechten
A. W. Schlechten
Head of Department

Golden, Colorado

Date: October 11 1965

ABSTRACT

An experimental method of determining dynamic flow stress from a total energy balance where the stress is homogeneous is developed using a pendulum bar-bar suspension system. A small specimen is mounted on the end of one of the bars and the other bar is impacted on the free end of the specimen.

For copper, the dynamic stress is 26% larger than the static stress for an increase in average strain rate of about five orders of magnitude. The increase in dynamic stress over the static value varied from 16% to 42%, which is comparable with the expected scatter for a typical test (24% to 38%) predicted from the uncertainties in measurement.

TABLE OF CONTENTS

Page

LIST OF ILLUSTRATIONS

LIST OF TABLES

LIST OF APPENDICES

ACKNOWLEDGEMENTS

The author is very grateful to Dr. J. D. Lubahn for his guidance and instruction during the course of this investigation. His analytical approach to practical problem solving was a great inspiration for the author's graduate studies and research.

The author is also indebted to Dr. A. W. Schlechten, Head of the Department of Metallurgical Engineering; Dr. R. S. Culver, Acting Director of Mining Research; and Mr. H. A. Babcock, Associate Professor of Basic Engineering for their assistance.

The author also wishes to acknowledge the financial support provided by the United States Air Force under contract number AF 29(601)6042.

INTRODUCTION

A considerable amount of research has been performed to investigate the effects of strain rate on stress, both as a function of strain and temperature. The present work was undertaken to investigate the effect of strain rate on stress at room temperature. The rates studied varied from 10^{-3}/sec., which was obtained from a Baldwin Lima Hamilton tension-compression testing machine, to 10^{2}/sec., which was obtained from the bar-bar pendulum impact machine.

The available dynamic tests from the literature are shown for copper in Tables 1 and 2. Copper was selected for this investigation because: (1) it has no energy absorbing phase transformation, (2) it is relatively free from impurities which may affect correlation with the work of others, and (3) it is commonly used for test purposes.

The data of the various investigators was compared by a ratio of the dynamic stress to the static stress, which provided a simple means of correlation. The dynamic stress was measured at the strain rate specified in Tables 1 and 2.

The tensile investigations of Manjoine & Nadai (1940), Baron (1956), and Culver (1963) showed good agreement between the stress ratios ($\pm$ 4.4% from the average of 1.15). The specimen geometries were similar; but the strain rates varied by a factor of 20, the strains varied by a factor of 100, and the load-measuring and strain-measuring devices were different in each case.

The investigations of Kolsky (1949), Bell & Werner (1962), and Davies & Hunter (1960) on dynamic compression behavior, however, do not agree. The stress ratio obtained by Kolsky is more than two, while Bell & Werner found that increasing the strain rate did not affect the stress at all. This difference in behavior exists even though the strains are the same in the three investigations and the strain rates are of the same order of magnitude.

Kolsky and Davies & Hunter obtained a strain rate effect in which the stress increased with increasing strain rate for constant strain. They both used the Hopkinson pressure bar with only slight modifications. Bell & Werner obtained no strain rate effect using the same strain and a higher strain rate than either Kolsky or Davies & Hunter. Bell & Werner did obtain a strain rate effect at 10% strain with a stress ratio of about 0.8. This value indicates that stress actually decreased with increasing strain rate in Bell & Werner's experiment.

The test set-up used by Bell & Werner differed from those of Kolsky and Davies & Hunter in that Bell & Werner did not use a thin wafer for a specimen and their approach for measuring and interpreting the load-strain curves was quite different (see Tables 1 and 2). Because of these serious discrepancies in the dynamic compression behavior of copper for various investigators, it was desirable to devise an experiment that would use a more direct method for measuring the stress and strain rate.

CHOICE OF IMPACT MACHINE

Of the three types of testing machines commonly used (bar-bar, bar-block, and block-block), the bar-bar machine was selected because: (1) the mechanics of impact can be explained quite precisely by simple theory, (2) the bar-bar machine is more stable dynamically than either the bar-block or the block-block machines, (3) alignment adjustments are easily made with the pendulum-type suspension system used, (4) this type of machine is very similar to the machines of the other investigators, and (5) an energy balance could easily be made on this system. The fact an energy balance can be easily applied to the bar-bar pendulum suspension system used for this experiment is necessary and will be analyzed first.

ENERGY BALANCE

An energy balance for constant total energy provides a method for the determination of dynamic stress. Writing such an energy balance for the bar-bar impact machine as shown in Figure 1, we obtain

$$PE_{iB} = PE_{iA} + PE_{sA} + E_{wf} + E_{wire} + E_{vib} + E_{pw} \tag{1}$$

For ease of nomenclature, the bar on which the specimen is mounted is termed the specimen bar (denoted by subscript s) and the other bar is termed the impacting bar (denoted by subscript i). Subscript B denotes conditions before impact, and subscript A denotes conditions after impact.

In Eq. (1) the total energy applied to the system is the potential energy of the impacting bar, PE_{iB}, before its release from a height above the initially stationary specimen bar. The potential energy of the specimen bar before impact is zero because the zero energy base of the system was chosen as the stationary height of the specimen bar.

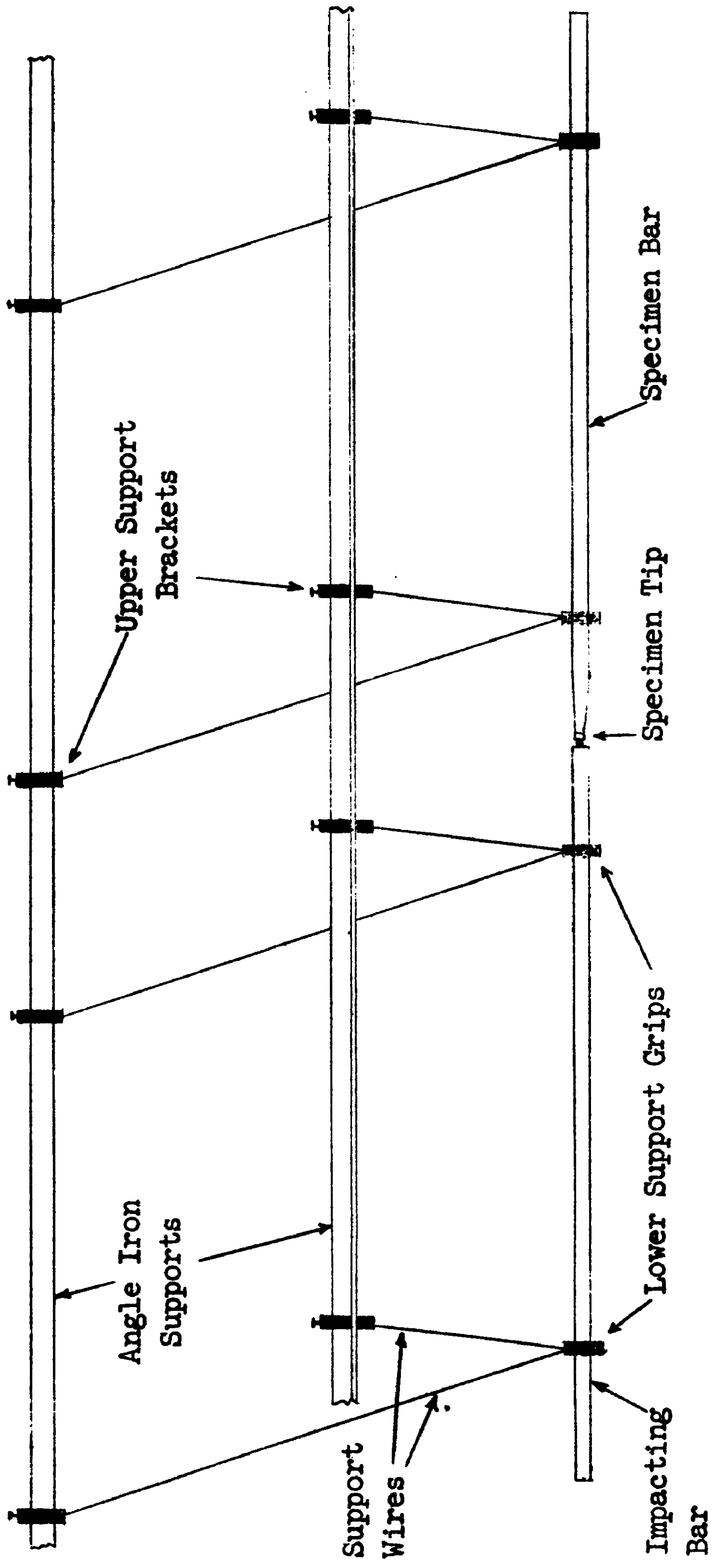

Figure 1. Pendulum Bar - Bar Impact Machine

PE_{iA} is the potential energy remaining in the impacting bar after the two bars have collided and separated. PE_{sA} is the potential energy remaining in the specimen bar after collision and separation have taken place. E_{wf} is the energy loss due to windage and friction. E_{wire} is the energy lost to the support wires. E_{vib} is the energy loss by vibrations of the bars after they have separated. E_{pw} is the energy available for plastic work of the copper specimen tip (small diameter portion of the specimen shown in Fig. 2). The plastic work is defined to include internal energy stored in the specimen and any heat that is transformed from this internal energy.

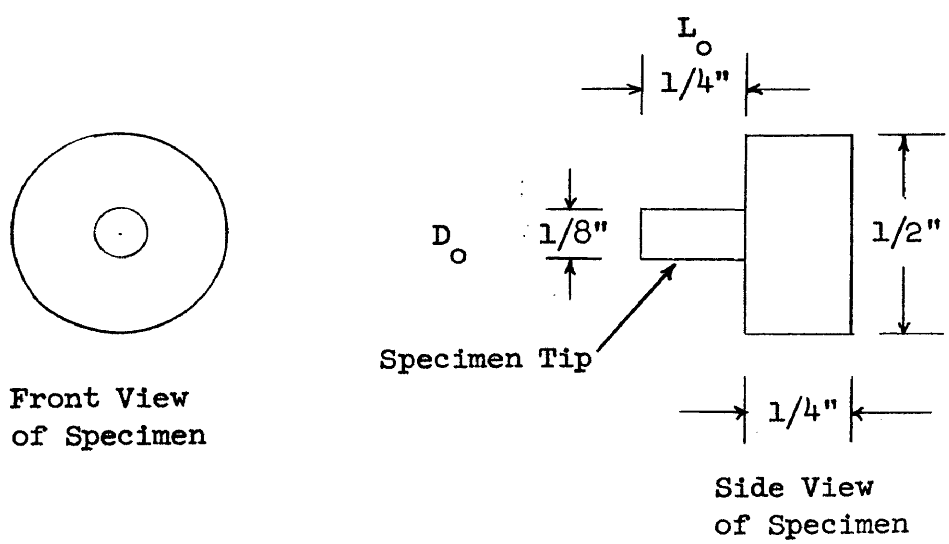

Figure 2. Test Specimen Dimensions

Plastic Work

A means of calculating the stress from Eq. (1) must be shown. To do this the last term of Eq. (1) involving the energy available for plastic work will be investigated.

The energy associated with plastic work is related to the applied impact load, P, the length, L_p, which is the final length of the specimen tip after the bars have separated, and the original length, L_o, of the specimen tip

$$E_{pw} = \int_{L_o}^{L_p} P \, dL \qquad (2)$$

Only plastic deformation is considered because the elastic part of the total deformation is transformed into potential energy and vibration loss and appears as energy of these forms in Eq. (1).

Eq. (2) is not in a very useful form so the following relations will be used: (a) the load, P, is equal to the true stress, S, times the instantaneous cross-sectional area, A; and (b) the infinitesmal change in plastic length, dL, is equal to the instantaneous length, L, times the infinitesmal logarithmic plastic strain in the longitudinal direction, de_p

$$P = SA \qquad (3)$$

$$dL = L\,de_p \,. \tag{4}$$

where the infinitesmal change in plastic length, dL, is the total infinitesmal length change minus the recoverable infinitesmal elastic length change. If (3) and (4) are substituted into (2) and the integration limits rewritten in terms of logarithmic plastic strain, the following relation is obtained

$$E_{pw} = \int_0^{e_p} ALS\; de_p \tag{5}$$

For plastic deformation the volume is a constant and the product AL may be removed from under the integral sign. The resulting equation divided by the volume (vol) of the specimen tip is

$$\frac{E_{pw}}{\text{vol}} = \int_0^{e_p} S\; de_p \tag{6}$$

For this investigation the integral of Eq. (6) can be easily evaluated since the essentially flat curve of true stress versus logarithmic plastic strain will be taken as horizontal (dashed line in Fig. 3) for both the static and dynamic cases. Thus, although the stress for a given strain may be higher for the dynamic case than for the static case, it is assumed that the stress is independent of e_p, and thus the

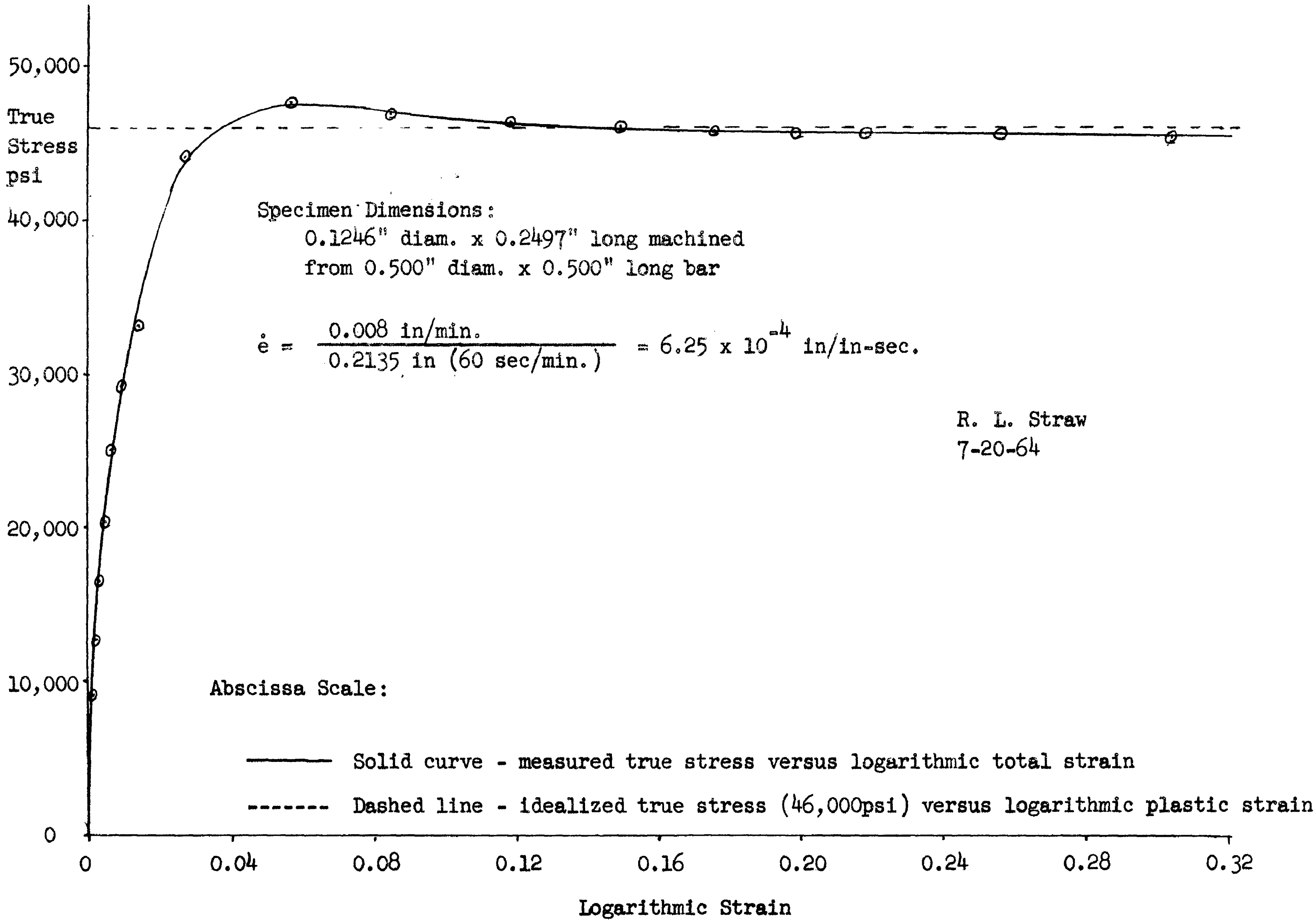

Figure 3. True Stress versus Logarithmic Strain for Tough Pitch Cold-Worked Copper

integral can be evaluated and the resulting expression rewritten to obtain

$$S = \frac{E_{pw}}{vol\ (e_p)} \tag{7}$$

The use of this equation requires that the dynamic stress is a constant for all logarithmic plastic strains. Eq. (7) is also limited by the requirement that the stress be distributed essentially uniformly over the length, L, considered. The purpose of this investigation is to determine whether this constant true stress will be equal to, less than, or greater than the static true stress as represented by the dashed line of Fig. 3.

The stress, S, can be obtained from the plastic work, E_{pw}, and the plastic work is found by difference from Eq. (1) after all the other terms have been measured. These terms are examined in the following sections to assure that all the energy losses can be measured and that an energy balance may be applied to the bar-bar impact machine with satisfactory results.

Potential Energy

The energy input to the system is the potential energy of the impacting bar before impact, PE_{iB}, which is equal to the weight of the impacting bar, w_{ib}, times the height, h_{iB}, it is raised above the initially stationary specimen bar

$$PE_{iB} = w_{ib}h_{iB} \tag{8}$$

The height of the impacting bar before its release, h_{iB}, is determined by measuring the zero level height and the height of the bar in the tied-back position by a vernier height gage. The height, h_{iB}, is the difference in these two heights.

The potential energies of the bars after impact were determined by measuring the arc lengths that the ends of the bars traveled. These arc lengths were then converted into bar heights by using Fig. 4. Fig. 4 represents the determination of arc length as a function of bar height both experimentally and analytically. The experimental determination of the relationship was conducted using a height gage to measure the height and a steel tape to measure the arc length. The equation for Fig. 4 is

$$h = \frac{(arc)^2}{136} \tag{9}$$

The arc length traveled by the impacting bar was measured with a horizontal ruler. Although this value is not actually the arc length, it is very close to the arc length since the radius of the path of travel

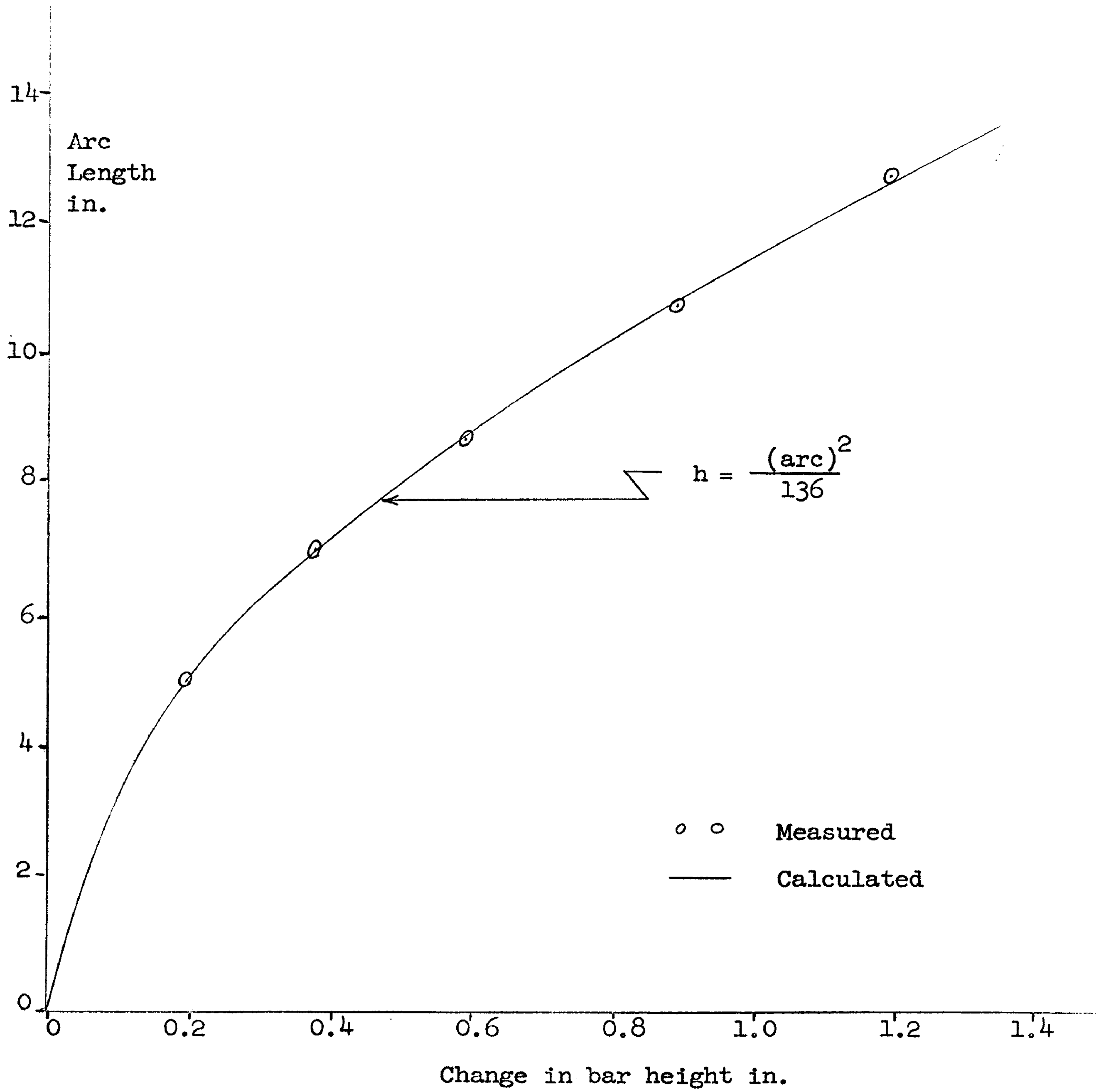

Figure 4. Arc Length Versus Change in Height for Both Bars

(68 in.) is quite large in comparison to the arc length (10 in.). The arc length of the specimen bar was measured by attaching a spring-mounted, ball point pen on the end of the bar. The trace of the ball pen was recorded on a trace board and the arc length was measured with a steel tape.

When the arc lengths and heights of both bars had been determined, the potential energies were evaluated from the following equations

$$PE_{iA} = w_{ib} h_{iA} \tag{10}$$

$$PE_{sA} = w_{sb} h_{sA} \tag{11}$$

where w_{ib} and w_{sb} are the weights of the impacting bar and specimen bar respectively (including the weight of their support blocks), and h_{iA} and h_{sA} are the heights that the impacting and specimen bars reached after impact.

Windage and Friction Loss

The windage and friction loss was measured by allowing each bar to swing freely (without colliding with the other bar) and recording the arc lengths from the base height of the bar to the starting point and return point. The starting and return points were recorded using the previously described ball pen and trace board. The two heights were obtained from Fig. 4 using the measured arc lengths. For a total arc length travel of 110.5 in. the energy loss due to windage and friction was 1.483 in-lb. The energy loss due to windage and friction was assumed to be proportional* to the arc length traveled. If the above experimentally measured values are used, the general expression for energy loss due to windage and friction, E_{wf}, is

$$E_{wf} = 0.01342 \text{ (total arc)} \tag{12}$$

where total arc is the total arc length for both bars.**

Wire Loss

The support wires may remove energy from the system while a test is in progress. In order to determine if any energy is removed and if so how much, a single support wire is considered separately from its bar support block. The potential energy of this wire in the pulled-back position is

$$PE_{wire} = w_{wire} \frac{h_b}{2} \tag{13}$$

where PE_{wire} is the potential energy of the wire, w_{wire} is the weight of the wire, and h_b is the height of fall of the lower end of the wire.

*For the relatively small variation of arc lengths involved in the tests.

**Subsequent tests show that windage and friction loss is much less than given by (12), but the vibration loss would then be greater by about the same amount and the plastic work would be essentially unchanged.

The kinetic energy of the wire when the potential energy is zero is

$$KE_{wire} = 1/2\ I_{us}\,\omega^2 \tag{14}$$

where I_{us} is the moment of inertia of the wire about the upper support and ω is the maximum angular velocity of the wire. If the potential and kinetic energies of the wire are equated and the following expression for I_{us} substituted

$$I_{us} = 1/3\ mL^2 \tag{15}$$

the following result is obtained

$$mg\,\frac{h_b}{2} = 1/2\ (1/3mL^2)\,\omega^2 \tag{16}$$

Simplifying (16) and noting that $L\omega$ is V_b, the velocity of the lower end of the wire, we find

$$V_b = \sqrt{3g\ h_b} \tag{17}$$

Now, if the bar is attached to the lower end of the wire, and the velocity at this point is again computed, the following expression results

$$V_b = \sqrt{2g\ h_b} \tag{18}$$

If equations (17) and (18) are compared, it can be seen that the wires do not remove energy from the system as was originally supposed. The wires actually add a very small energy to the system. On the other hand, this small energy is included in the windage and friction term of Eq. (1) because of the way in which this term was determined experimentally, and so Eq. (1) reduces to

$$PE_{iB} = PE_{iA} + PE_{sA} + E_{wf} + E_{pw} + E_{vib} \tag{19}$$

Vibration Loss

The energy loss due to vibrations of the bars after impact, E_{vib}, is difficult to measure when plastic work is done in the system. To estimate this value the vibration losses for an elastic test can be measured instead, and a suitable method used to relate the vibrations and energy loss in the elastic test with those of any plastic test. The strains resulting from vibrations at the midpoint on one of the bars can be measured and provide a method for correlating vibrational energy loss after impact for elastic and plastic tests.

Ideal Elastic Impact

To aid in understanding this energy loss a brief discussion of bar-bar impact and the resulting vibrations is presented. The ideal case of the collinear impact of two cylindrical bars of equal length and cross-section with plane ends will be described for elastic conditions. The specimen bar is initially at rest and the impacting bar is at a height, h_o, which will give it a velocity of V_o (found by equating potential and kinetic energies for the bar) just before the two bars collide.

For a time on the order of 10^{-4} second after collision has taken place the impacting surface between the two bars and a short length of each bar adjacent to the point of impact will be traveling at a velocity of one-half V_o. This velocity can be obtained by writing a momentum and a kinetic energy balance for corresponding elements of each bar near the impacting surface before collision and for a short time after the collision has commenced. After a time equal to the length of one bar divided by the velocity of sound in the bar (approximately 3×10^{-4} sec.), the velocities of every part of both bars will be one-half V_o and every part of both bars will be strained equally in compression.

The bars now return to their original unstrained lengths by changing velocity at the free ends. The velocity of the specimen bar at the free end increases to V_o, and the free end of the impacting bar decreases to zero velocity. These velocities are again obtained from a momentum and kinetic energy balance for a time just less than and just greater than the length of one bar divided by the velocity of sound in the bar. The velocity o the remaining portion of the specimen bar increases to V_o as the bar returns to its initial length until the whole bar is at velocity V_o. When the impacting bar has returned to its initial length, the velocity of the entire bar is zero.

The instant both bars have returned to their original lengths, the impacting surfaces separate. The bars have exchanged velocities with each other from their initial values. Thus there are no residual vibrations present in the bars for this ideal case.

Actual Elastic Impact

For the actual impact of two bars, a small fraction of the initial longitudinal vibrations are present after impact because of differences in length and weight of the bars and from non-planar impact conditions. Most of the lateral vibrations also remain after impact and result from any one or more of the following factors: (1) the bars are not perfectly straight, (2) the bars are not concentric, (3) the bars are not aligned, (4) the bars do not swing parallel to each other, and (5) the paths of the swinging bars do not describe a vertical plane. The lateral vibrations can be minimized by careful attention to these details, however these losses are difficult to eliminate completely and so must be determined by a suitable combination of measurement and analysis such that the term E_{vib} in Eq. (19) can be evaluated. The vibration loss, E_{vib}, for the non-ideal elastic impact of two bars is obtained by summing the lateral, E_{Lat}, and longitudinal, E_{Long}, components of the vibration loss

$$E_{vib} = E_{Lat} + E_{Long} \tag{20}$$

where the lateral and longitudinal vibration losses are independent of each other and are proportional to the amplitude of the lateral and longitudinal strains respectively.

Plastic Impact

The description of the impact for the plastic case is complicated by the presence of a yielding link between the impact surfaces of the elastic bars previously described. This complication is caused by several factors: (1) the changes in the length of the specimen bar do not take place until the specimen itself has been deformed, (2) the specimen may bend in addition to decreasing in length, and (3) the time required for transmission of the deformation through the specimen is not known.

Four assumptions will be made in estimating the vibration losses for a plastic test: (1) the primary mode of lateral vibrations is the first mode, (2) the vibrations in both bars are identical for a given test, (3) the longitudinal strain is uniform over the length of either bar, and (4) the distribution of lateral and longitudinal vibrations in the bars is similar for both an elastic test and any plastic test when the test geometries are identical. The same theory for prediction of vibration loss in an elastic test, given by Eq. (20), may therefore be used for the plastic tests.

Longitudinal Vibration Loss

The energy loss resulting from longitudinal vibrations after the bars have separated can be determined when the potential energies of the vibrating bars are maximum. This occurs when the bars have stretched to a maximum length or shortened to a minimum length. This energy loss is

$$E_{long} = \int_{l_o}^{l_{max}} SA\ dl \qquad (21)$$

The infinitesmal change in length, dl, is proportional to the infinitesmal change in longitudinal strain, de_l, by

$$dl = l - l_o = l_o\ de_l \qquad (22)$$

The stress, S, is related to the strain from Hooke's Law as

$$S = Ee_l \qquad (23)$$

If Eqs. (22) and (23) are substituted into (21) and the limits of integration rewritten in terms of strain the energy loss due to longitudinal vibrations becomes

$$E_{long} = \int_0^{e_{long}} EAl_o\, e_l\, de_l \tag{24}$$

where e_{long} is the maximum strain in the longitudinal direction. Since Young's Modulus, E, is constant and the area and length of the bars are essentially constant, Eq. (24) can be integrated. If the volume ($2\,Al_o = VOL$) of both equally vibrating bars is substituted for the volume of one bar in Eq. (24) and the integral is evaluated, the longitudinal vibration loss for both bars is

$$E_{long} = \frac{E\, e_{long}^{2}\, VOL}{2} \tag{25}$$

The longitudinal strain e_{long} of Eq. (25) and the lateral strains described in the following section were determined from four semi-conductor strain gages wired in opposite pairs and mounted axially in the center of the specimen bar. The outputs from each of the two pairs of gages were fed to separate amplifiers and then in turn to separate oscilloscopes. Photographs of the oscilloscope strain gage outputs were made with Polaroid oscilloscope cameras and the strains were determined from the amplitudes as recorded on the photographs. The details of the strain gage wiring and the calculation of the strain from the strain amplitude can be found in the section entitled "Strain Measurement."

Lateral Vibration Loss

The energy loss resulting from lateral vibrations of the bars after impact can be determined analytically only for a particular small finite length of the bar where the maximum lateral surface strain, e_g, is known

$$E_{lat} = \int_0^{\delta} \int_0^{F} dF \, d\delta \tag{26}$$

In Eq. (26) dF is the force on an element dx thick, Δl_o long, and distance x from the neutral axis as shown in Fig. 5

$$dF = S \, dA \tag{27}$$

The infinitesmal change in length $d\delta$ is

$$d\delta = \Delta l_o \, de \tag{28}$$

where de is the infinitesmal change in lateral strain at distance x from the neutral axis when the surface strain is e_s $(e_s < e_g)$.

The force on element dx can be found from the definition of Hooke's law for uniaxial loading

$$S = Ee \tag{29}$$

and from the geometry of Fig. 5

$$e = e_s \frac{x}{R} \tag{30}$$

and

$$dA = 2\sqrt{R^2 - x^2} \, dx \tag{31}$$

If (29), (30), and (31) are combined with (27) and the result substi-

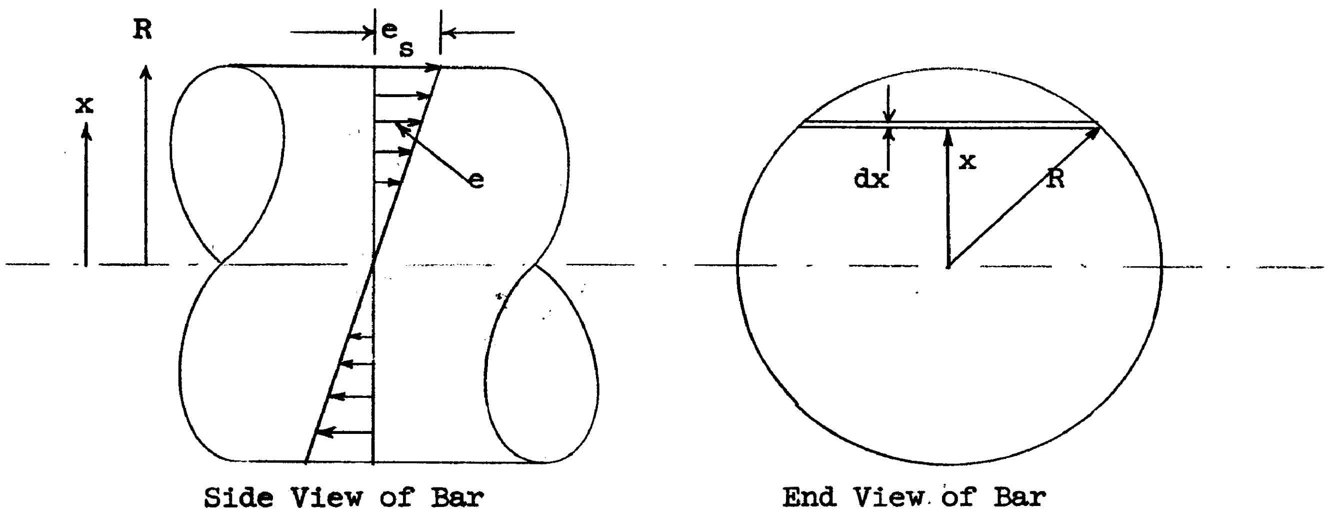

Figure 5. Lateral Strain Distribution in a Round Bar

tuted into (26) the lateral vibration energy loss for a particular short length of one vibrating bar is

$$E_{lat} = \int_0^{\delta} 2\int_0^{R} \frac{Ee_s\,x}{R}\, 2\sqrt{R^2 - x^2}\, dx d\delta \qquad (32)$$

If (30) is differentiated with respect to both strains holding x constant and then substituted into (28), the lateral vibration energy loss from (32) becomes

$$E_{lat} = \int_0^{e_g} 2\int_0^{R} \frac{2E\Delta l_o\, x^2}{R^2}\sqrt{R^2 - x^2}\, dx\, (e_s de_s) \qquad (33)$$

Integrating (33) with respect to lateral surface strain e_s and substituting the proper limits we have

$$E_{lat} = \frac{e_g^2}{2}\, 2\int_0^{R} \frac{2E\,\Delta l_o}{R^2}\, x^2\sqrt{R^2 - x^2}\, dx \qquad (34)$$

Integrating now with respect to x, we obtain the lateral vibration loss for a short length of bar

$$E_{lat} = 0.0983\, E\,\Delta l_o\, e_g^2\, R^2 \qquad (35)$$

The lateral strain, e_{lat}, measured from the oscilloscope recordings of the output from two of the semiconductor strain gages placed in adjacent arms of a Wheatstone bridge is twice the maximum surface strain e_g of Eq. (35) because the output strains of the two gages are added when the lateral strain is a maximum.

$$e_g = \frac{e_{lat}}{2} \tag{36}$$

The lateral strain energy loss for a particular short length of a bar is then

$$E_{lat} = 0.0246\ E\ \Delta l_o\ R^2\ e_{lat}^{\ 2} \tag{37}$$

The energy loss due to lateral vibrations for a short length of a bar is directly proportional to the measured lateral surface strain squared. The lateral strain distribution along the length of the bar is unknown, but the lateral vibration energy loss can still be evaluated in terms of the measured lateral strain if the total energy loss for both bars is proportional to the measured strain squared

$$E_{lat} = C\ (e_{lat})^2 \tag{38}$$

Eq. (38) applies if the assumption is made that the distribution of lateral strains varies only in magnitude when the results of different tests are compared.

Since only the lateral strain amplitude, Am_{lat}, is obtained directly from the pictures of the oscilloscope outputs of the strain gages, Eq. (38) could be more easily evaluated if the lateral vibration energy loss could be determined from the lateral strain amplitude. But the lateral strain is directly proportional to the lateral strain amplitude, and so the substitution can be made with only the proportionality constant C in Eq. (38) changing to K_1

$$E_{lat} = K_1 \, (Am_{lat})^2 \tag{39}$$

The description of the strain measuring equipment and layout is required for the understanding of how the strains were determined.

Strain Measurement

Eqs. (25) and (39) give a method for the determination of the energy losses due to vibrations. The previously mentioned elastic test provides a method for the determination of constant K_1 of Eq. (39). A description of the equipment used for the determination of e_{long} and Am_{Lat} is required for the explanation of how constant K_1 was determined and how the subsequent components of the vibrational energy loss were obtained for any plastic test.

Four, Baldwin Lima Hamilton, SR-4 Type, semiconductor strain gages were mounted longitudinally in the center of the specimen bar on both sides, top, and bottom. Semiconductor strain gages were used because their unusually high sensitivity (55 times the normal gage factor of 2) was necessary for the proper amplification of the small strains encountered (approximately 20×10^{-6} in/in). The center of the bar was chosen because the first mode of lateral vibrations was expected to predominate over the other modes.

The use of only four gages limits the number of strains that can be measured at any one time. The horizontal component of the lateral strain was always measured using the two opposite side gages, but the top and bottom gages were sometimes used for longitudinal strain and sometimes for measuring the vertical component of lateral strain. The side gages were wired into one Wheatstone Bridge circuit and the top and bottom gages were wired into a second Wheatstone Bridge circuit. Provision was made so that both the top and bottom gages could be placed in one arm of the circuit in series, which would allow the longitudinal pulse and vibrations to be measured, or be placed in adjacent arms of the bridge circuit, which would allow the lateral vibrations to be measured. The gages on the sides of the specimen bar were left in opposite arms of their Wheatstone Bridge circuit to measure the horizontal component of the lateral vibrations for each test.

The outputs for both pairs of gages were fed into separate amplifiers. The amplifier outputs were fed to separate oscilloscopes equipped with Polaroid oscilloscope cameras to record the vibration traces. A sketch for a typical longitudinal trace and a lateral trace is shown in Fig. 6.

The maximum longitudinal strain is obtained by measuring the largest amplitude of any of the peaks after the first two (which represent

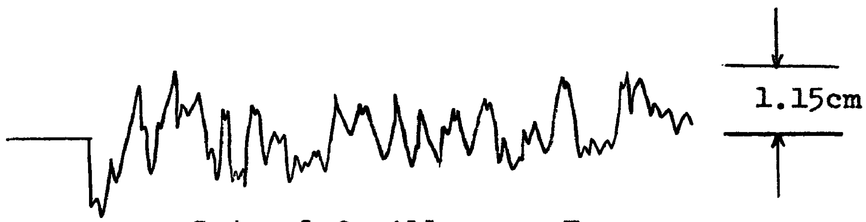

Lateral Oscilloscope Trace
(Test Number 15)

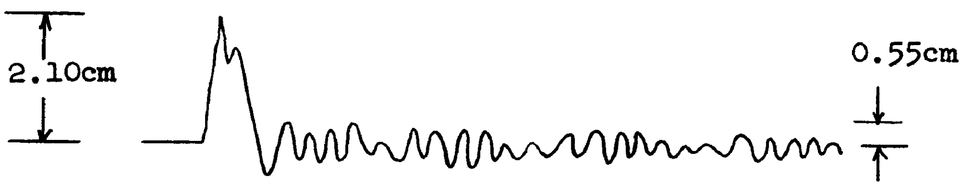

Longitudinal Oscilloscope Trace
(Test Number 11)

Figure 6. Traces of Oscilloscope Photographs of Strain Gage Output

pulsations in the bar while the two bars were still in contact--see Fig. 6.) The strain causing this maximum longitudinal peak is given by the following expression

$$e_{Long} = \frac{2VS\ Am_{Long}}{RIK} \tag{40}$$

where e_{Long} is the maximum longitudinal strain, VS is the vertical sensitivity of the oscilloscope (volts/cm), Am_{Long} is the maximum longitudinal trace of strain amplitude after bar separation (cm), R is the resistance of two of the strain gages together in ohms, I is the current in the circuit (amps), and K is 110, the gage factor (amplification factor) of the strain gages.

Determination of Vibration Losses

The maximum lateral and longitudinal strain amplitudes were obtained from strain gage output recordings like Fig. 6. The maximum longitudinal strain was found by substituting the following quantities into Eq. (40) -- (1) the vertical sensitivity was 0.005 volts per centimeter, (2) the total resistance of two gages was 240 ohms, and (3) the current was 0.040 amperes

$$e_{Long} = 9.47 \times 10^{-6}\ Am_{Long} \tag{41}$$

Now the evaluation of constant K_1 can proceed. The elastic test used for this purpose duplicated the specimen gemoetry of the plastic tests except for the replacement of the usual copper specimen with a hard steel specimen (yield strength > 100,000psi). The steel specimen did not deform plastically in this test so Eq. (19) is modified for this case as follows

$$PE_{iB} = PE_{iA} + PE_{sA} + E_{wf} + E_{vib} \tag{42}$$

If the data for test A-2 with the hardened steel tip (Tables 3 and 4) is used in the evaluation of the vibration loss in Eq. (42), the vibration loss is calculated to be 1.13 in-lb. The longitudinal vibration loss for test A-1, which is the same as for test A-2, was calculated using (25) and (40) as 0.02 in-lb. The lateral vibration loss was then evaluated using the following relation obtained from Eq. (20)

$$E_{lat} = E_{vib} - E_{Long} \tag{43}$$

For this elastic test, the loss due to lateral vibration was then 1.11 in-lb.

In order to determine K_1 for Eq. (39), the maximum amplitude of the lateral strain trace must be obtained. This is given by

$$Am_{Lat} = \sqrt{Am_{vert}^{2} + Am_{horiz}^{2}} \tag{44}$$

where Am_{vert} and Am_{horiz} are the maximum amplitudes measured from the

where Am_{vert} and Am_{horiz} are the maximum amplitudes measured from the

Am_{vert} of 1.40cm and Am_{horiz} of 1.00cm the maximum lateral amplitude, Am_{Lat}, from Eq. (44) is 1.72cm. When this value is substituted into Eq. (39) along with the calculated value of the lateral vibration energy loss (E_{Lat} = 1.11 in-lb), constant K_1 is found to be 0.375 in-lb/cm^2. It must be noted that this value is based on the assumption that the lateral strain distribution differs only in magnitude when elastic test results are compared with plastic results. Eq. (39) then becomes

$$E_{Lat} = 0.375 \, (Am_{Lat})^2 \tag{45}$$

Eqs. (25) and (45) give the longitudinal and lateral vibrational energy losses for any test. Since there are only two plastic tests in which the longitudinal strain amplitude was measured, the energy loss due to longitudinal vibrations is assumed to be the same for all the plastic tests. If the longitudinal amplitude of 0.525cm (found by averaging the longitudinal amplitudes of tests 5 and 11--Table 3) is substituted into Eq. (41) the longitudinal strain, e_{Long}, is 2.61 x 10^{-6} in/in and the longitudinal energy loss from (25) is

$$E_{Long} = 0.02 \text{ in-lb} \tag{46}$$

If (46) is substituted into (20), the vibrational energy loss is

$$E_{vib} = 0.02 + E_{Lat} \tag{47}$$

The energy available for plastic work can now be obtained by modifying Eq. (19) to yield

$$E_{pw} = PE_{iB} - PE_{iA} - PE_{sA} - E_{wf} - E_{vib} \tag{48}$$

The quantities on the right hand side of Eq. (48) are summarized as follows

$$PE_{iB} = w_{ib}\ h_{iB} \tag{8}$$

$$PE_{iA} = w_{ib}\ h_{iA} \tag{10}$$

$$PE_{sA} = w_{sb}\ h_{sA} \tag{11}$$

$$E_{wf} = 0.01342 \text{ (total arc)} \tag{12}$$

$$E_{vib} = 0.02 \text{ in-lb} + E_{Lat} \tag{47}$$

$$E_{Lat} = 0.375\ (Am_{Lat})^2 \tag{45}$$

DETERMINATION OF STRAIN

The stress can be evaluated from Eq. (7) after the strain and volume have been determined. The volume of the specimen tip was calculated from the original dimensions of the copper specimen tip (1/8" diam. x 1/4" long nominally). The logarithmic plastic strain in the axial direction is most reliably* determined by first calculating the logarithmic plastic strain in the radial direction, e_r, given by the following formula

$$e_r = \frac{D_{ave}}{D_o} \tag{49}$$

where D_{ave} is the average diameter** after impact (determined by measuring the diameter at 0.01" intervals along the axis of the deformed

---

* Diameter measurements are preferred over length measurements for this purpose because of the larger number of diameter measurements and other considerations of reliability.

** The degree of nonuniformity of diameter is given in Table 5.

tip and dividing the sum of these diameter readings by the number of readings), and D_o is the initial diameter of the specimen tip. The diameter after impact readings were obtained by using the 0.0001" dial strain gages fitted with small rounded points.

The logarithmic strain, e_p, can then be evaluated using the constant volume condition for the plastic case

$$e_p = -2\ e_r \tag{50}$$

DETERMINATION OF STRAIN RATE

The strain rate $\dot{e}$ is defined as the strain divided by the time of straining t

$$\dot{e} = \frac{e_p}{t} \tag{51}$$

The strain is given by Eq. (50) and the time for straining is determined by equating impulse and momentum for either bar. The strain rates obtained in this manner should be independent of the bar chosen for equating impulse and momentum

$$F\ (t) = m\,\Delta v \tag{52}$$

In this equation F is the force on the specimen tip and is equal to the final area of the specimen tip A times the maximum average stress in the tip S

$$F = SA \tag{53}$$

m is the mass of the bar, and Δv is the change in velocity of the bar.

For the impacting bar, the change in velocity Δv is given by the initial velocity before impact

$$v_{iB} = \sqrt{2g\ h_{iB}} \tag{54}$$

minus the velocity after impact

$$v_{iA} = \sqrt{2g\ h_{iA}} \tag{55}$$

The strain rate based on equating impulse and momentum for the impacting bar is

$$\dot{e} = \frac{e_p\ SA}{m_i\left(\sqrt{2g\ h_{iB}} - \sqrt{2g\ h_{iA}}\right)} \tag{56}$$

where m_i is the mass of the impacting bar.

By equating impulse andmomentum for the specimen bar and noting that the velocity of the specimen bar after impact is

$$v_{sA} = \sqrt{2g\ h_{sA}} \tag{57}$$

we find the strain rate

$$\dot{e} = \frac{e_p \, SA}{m_s \sqrt{2g \, h_{sA}}} \tag{58}$$

in which m_s is the mass of the specimen bar.

The sample calculations (Appendix 1) for strain rate by both (56) and (58) show that the two values which should be identical are actually only with 10% of each other. For simplicity the remaining strain rates were obtained only from Eq. (56) although Eq. (58) could have been used instead.

DESCRIPTION OF EQUIPMENT

Now that the method for the determination of stress, strain, and strain rate has been presented, the experimental apparatus not previously described is explained. This explanation is necessary as a prelude to the description of how a typical test was run and how the control of alignment was assured.

Specimens

All test specimens consisted of copper tips machined from one piece of tough pitch (99.2+% pure), cold-rolled, copper round machined according to the nominal dimensions specified in Figure 2. The specimens were glued on the end of the specimen bar with Eastman 910 glue and a glue accelerator. A length to diameter ratio of 2 was used to prevent undue transverse restraint of the specimens (appears when L/D is less than 2) and to prevent buckling (which is caused by using

L/D of greater than 2). Early difficulty with buckling of the specimens was experienced when an effective L/D ratio of four was used.

Bars

The impacting bars were constructed from six-foot lengths of 3/4" diameter, SAE 1018, cold-rolled steel. The impacting end of the specimen bar was tapered down to 1/2" diameter over a six inch length for ease of centering the specimens. The end of the impacting bar was fitted with a hard steel disk (yield strength > 100,000psi) which protected the end of the bar from being plastically deformed.

Support Grips and Wires

Hand bent and rough machined bar grips caused a great deal of alignment trouble and bar mounting problems in tests preliminary to those summarized in Tables 3 and 4. The construction of identical, precision-made bar grips, as shown in Fig. 7, eliminated this problem. The linen twine used in early tests for support material was changed to 70" long, 1/16" diam., steel wires with 0-80 threads on each end. These threads provided a means of adjustment of the length of the wires which were secured to the bar supports and upper wire supports by pairs of adjustable lock nuts.

Ball bearings were mounted in the extended upper arms of the Y-

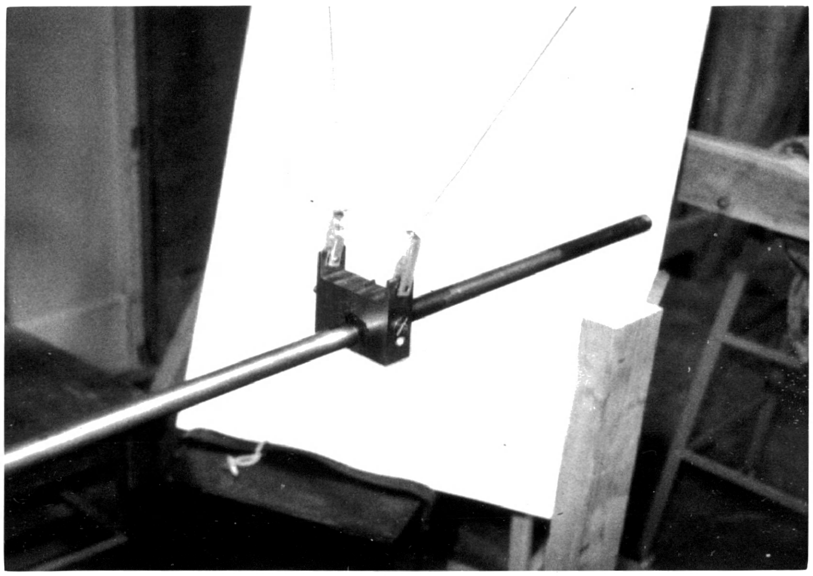

Figure 7. Specimen Bar, Grips, and Lower Wire Mountings

shaped, lower bar grips and in the upper wire supports. The wires were fastened to the yokes which pivoted with respect to the vertical adjustment pins as shown in Figs. 7 and 8. This construction allowed the wires to swing freely with minimum friction loss and no wire bending.

Upper Supports and Adjustments

To provide fine adjustment for the bars, the wires were suspended from special three-directional adjustment gages. The upper supports consisted of microscope stages, which possessed two degrees of horizontal freedom, mounted to the angle iron supports by hand tightened screws. On the ends of the microscope stages were mounted specially constructed vertical adjustment devices held in place by two bolts as shown in Fig. 8. When final adjustments were completed on the upper supports, the microscope stages were fastened to the angle iron supports by means of C-clamps to prevent any motion during testing.

Support Frame

The angle iron bars were rigidly mounted to a wooden 2 x 4 frame which supported the 12 foot span of the angle irons at both ends and the middle. The wooden frame was cross-braced at both ends and one side and the remaining side was bolted rigidly to a support wall. This was done to prevent movement of the frame during testing.

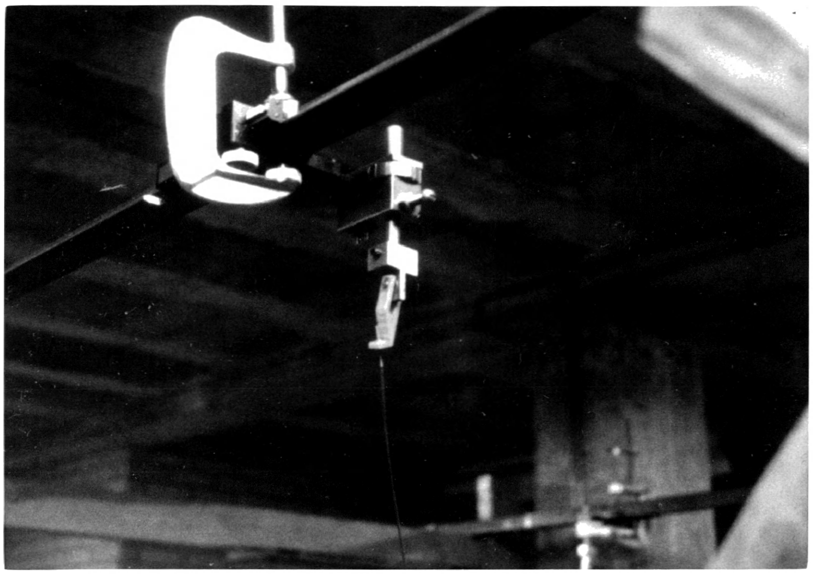

Figure 8. Upper Support and Microscope Stage Mounting

EXPERIMENTAL PROCEDURE

The experimental test procedure is described in the following sections. A test procedure and data sheet (Fig. 9) is included to show the information recorded during an actual test run. Explanation required for steps 2, 3, 4, and 12 of the procedure sheet is included below. An explanation of the height measuring techniques is to be found in the description of the energy balance.

Preliminary Alignment

The proper alignment of the bars is required to minimize the vibration losses and to eliminate transverse bending of the specimen tip. The axes of the bars must be coincident when they are at rest. As the bars swing, they remain horizontal and must travel in the same vertical plane. To this end, the support wires must be perpendicular to the axes of the bars when they are at rest.

IMPACT TEST PROCEDURE

Test no. 12 Date Aug. 21, 1964

Specimen Material Copper

	check when completed	initial reading	final reading
1. measure specimen dimensions	✓	L_{total} .6687	.6450
2. align bars with three transits	✓	$-L_{thick}$ .4125	.4125
3. glue specimen on tip using sleeve	✓	L_{spec} .2562	.2325
		Diam .1247	.1322
4. adjust pen and trace paper	✓	h_{high} -	
5. measure differential height, Δh, of impacting bar	✓	$-h_{low}$ -	
		Δh 5.00	
6. set strain gage current	✓	Current = 40 ma	
7. check position of oscilloscope trace	✓	Lateral trace 2	
8. check type of trace picture(s) taken	✓	Longitudinal trace none	
9. record oscilloscope settings	✓	oscilloscope sweep speed 2 ms/cm	
10. check and set trigger	✓	oscill. vertical sensitivity .005 v/cm	
11. release bar with match	✓	specimen bar arc 12⅜ in	
12. record arc lengths traveled by both bars after impact	✓	impacting bar arc 7 in	
13. record final specimen dimensions	✓	TEST COMMENTS none	

Picture of horizontal lateral trace Picture of vertical lateral trace

Figure 9. Sample Test Data Information Sheet

The four upper pivot points for each bar were squared and leveled. This was achieved by measuring opposite spans with a steel tape and setting them equal. The longitudinal distances (parallel to the bars' axes) of the upper supports were set equal to the distance between the grips on the bars. The diagonals were then measured and set equal. After the horizontal adjustments were clamped and fixed, the upper support points were made horizontal by adjusting the vertical motion of the four upper support points for each bar. A transit was used to determine if all eight upper support points were horizontal. When the upper support points had been adjusted according to this procedure, they were not adjusted again since it was found in practice that they did not move after many tests.

Three additional transits were used to align the bars. Lines 90° apart were scribed on both ends, and the sides, top, and bottom of both bars for such alignment. The bars were leveled with two transits using the horizontal lines on the sides of the bars for a guide. The nuts on the lower ends of the support wires were used to align the bars. The bars were placed in the same vertical plane with the third transit by using the lines on the ends and the tops of the two bars for guides.

Mounting the Specimen Tip

The specimen tips were mounted by using a cylindrical sleeve that fitted over the impacting bar on one end and was machined on the other end to hold the barrel of the specimen. The tip was placed in the sleeve and Eastman 910 glue applied to the back. Accelerator was then spread on the impacting end of the specimen bar and the specimen and specimen bar were pressed together. As soon as the tip was securely mounted, the alignment sleeve was removed and the test was ready to proceed. This procedure assured concentricity of the specimen tip and impacting bar.

Alignment of Ball Pen and Trace

The alignment of the ball pen, mounted on the end of the specimen bar, and the trace board were checked; and the board was positioned so that a minimum tracking force was applied to the ball pen.

Release of Impacting Bar

Before releasing the impacting bar, all the steps on the alignment procedure sheet were checked to be sure all necessary pre-test information was recorded. The impacting bar was then released from its initial position by burning the tie-back string with a match.

TEST DATA AND CALCULATIONS

A sample calculation for the stress and strain rate for a typical test (test #12) is shown in Appendix 1. A sample experimental data sheet is shown in Fig. 9 with the test information for test 12 inserted as a sample of the recorded information. The determination of the vibration loss for each test is summarized in Table 3. The determination of the energy available for plastic work is summarized in Table 4. The determination of plastic strain for each test can be found in Table 5. The values of stress, strain, and strain rate for each test are in Table 6.

ERROR ANALYSIS

The calculations for the error analysis (Table 7) are based on the uncertainties in the measuring equipment used. A typical test (test #12) was analyzed for the uncertainties in the determination of the plastic work, strain, volume, and the stress resulting if these errors are allowed to reach their maximum values simultaneously. In the case of test #12, for a 0.44 in-lb error in available energy, a 0.0016 error in strain, and a 5×10^{-6} in^3 error in volume, the stress can be in error as much as $\pm$ 3,300 psi.

TEST RESULTS AND CONCLUSIONS

The test results are tabulated in Table 6. The ratios of the dynamic to static stresses and strain rates were used to compare the results of the present experiments with each other and with the results of the other investigators.

The average stress ratio was 1.26 and the average strain rate ratio was $10^{5.19}$. The stress ratio varied from 1.16 to 1.42. Error analysis of a test near the median (test #12) showed that the stress ratio could be expected to vary from 1.24 to 1.38. Thus, the experimental scatter is comparable with the spread between the extreme values from the error analysis. There is an average strain rate effect of 26% increase, and at least 16%, even for the lowest experimentally measured stress, for a change in strain rate of more than five orders of magnitude.

The results of the present investigation are compared with the results of the other investigators (data from Tables 1 and 2) in Fig. 10. The present dynamic results, together with the dynamic results of Culver, Baron, and Davies & Hunter, fall on a single trend line. Nadai & Manjoine and Kolsky also found a rate effect, one effect being higher, and the other being lower, than the trend line. Bell & Werner disagree with all other investigators in that they found no rate effect.

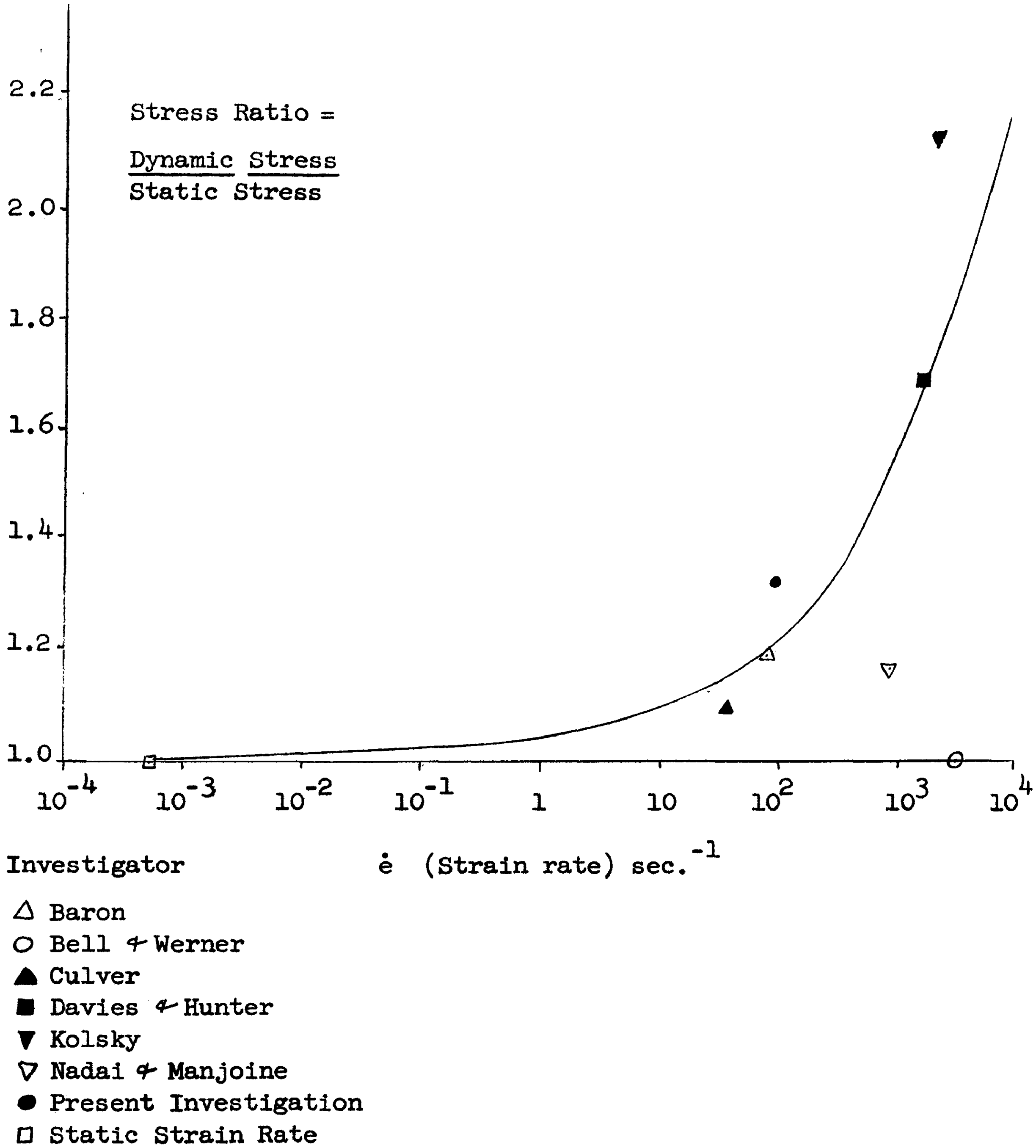

Figure 10. Stress Ratio Versus Strain Rate for Pure Copper from Various Investigators

Table 1. Previous Tension Impact Investigations

AUTHOR	Manjoine & Nadai (1940)	Baron (1956)	Culver (1963)
TEST MECHANISM	block-block	block-block	block-bar
ENERGY SOURCE	flywheel	Charpy pendulum	spring
LOAD MEASUREMENT	from elastic strain in rigid steel bar	weighbar with strain gages	from elastic strain in rigid steel bar
STRAIN MEASUREMENT	relative motion between two heads	calculated from force-time curve	drum camera and scribed lines on specimen
MATERIAL	annealed copper	annealed copper	annealed copper
SPECIMEN DIMENSIONS	solid 0.200" diam. by 1-1/8" long	solid 0.138" diam. by 0.75" long	solid 0.200" diam. by 1" long
DYNAMIC STRAIN RATE	900/sec.	90/sec.	45/sec.
DYNAMIC STRESS/ STATIC STRESS	1.15	1.2	1.1
METHOD OF DATA PRESENTATION	Stress versus strain for different rates	Stress versus strain for given rate	Stress versus strain-time plotted on same axis
STRAIN	20% elastic plus plastic	0.2% plastic	10% elastic plus plastic

Table 2. Previous Compression Impact Investigations

AUTHOR	Kolsky (1949)	Bell & Werner (1962)	Davies & Hunter (1960)
TEST MECHANISM	bar-bar	bar-bar	bar-bar
ENERGY SOURCE	explosive charge	air gun	explosive charge
LOAD MEASUREMENT	cylindrical condenser microphone	calculated from strain-time curve	numerical analysis of displacement-time curve
STRAIN MEASUREMENT	parallel plate condenser microphone	diffraction grating with mercury arc	capacitance discharge with and without specimen
MATERIAL	annealed copper	annealed copper	annealed copper
SPECIMEN DIMENSIONS	solid 1" diam. by 0.05cm thick	solid 0.990"diam. by 10" long	solid 1" diam. by 0.3" thick
DYNAMIC STRAIN RATE	2000/sec.	3660/sec.	1100/sec.
DYNAMIC STRESS/ STATIC STRESS	2.1	1.0	1.67
METHOD OF DATA PRESENTATION	Stress versus strain for given rate	Stress versus strain for given rate	Stress versus strain for given rate
STRAIN	1.5% elastic plus plastic	1.5% elastic plus plastic	1.5% elastic plus plastic

Table 3. Strain Gage Amplitudes and Vibration Losses

Test No.	Am_{horiz} cm	Am_{vert} cm	Am_{Lat} cm	Am_{Long} cm	E_{Lat} in-lbs	E_{Long} in-lbs	E_{vib} in-lbs
5	2.15	1.35*	2.54	0.50	2.41	0.02	2.43
7	2.50	0.65	2.60	-	2.52	0.02	2.54
8	1.60	1.10	1.94	-	1.42	0.02	1.44
11	1.40	1.35*	1.95	0.55	1.42	0.02	1.44
12	1.30	1.35	1.87	-	1.32	0.02	1.34
13	1.05	1.35*	1.71	-	1.09	0.02	1.11
14	1.15	1.35*	1.77	-	1.17	0.02	1.19
15	1.15	0.85	1.43	-	0.76	0.02	0.78
16	1.80	1.00	2.06	-	1.60	0.02	1.62
A-1	1.25	-	-	0.50	-	0.02	-
A-2	1.40	1.00	1.72	-	1.11	0.02	1.13

*Assumed value needed for the purpose of calculating Am_{Lat}

Table 4. Determination of Energy Available for Plastic Work

Test No.	h_{iB} in.	arc iA in.	arc sA in.	PE_{iB} *1 in-lb	PE_{iA} *1 in-lb	PE_{sA} *2 in-lb	E_{wf} in-lb	E_{vib} in-lb	E_{pw} in-lb
5	5.00	9 1/4	16 13/16	61.10	7.69	24.48	0.70	2.43	25.80
7	5.00	9	15 1/4	61.10	7.28	20.14	0.68	2.54	30.46
8	5.00	9 1/4	14 1/2	61.10	7.69	18.21	0.67	1.44	33.09
11	5.00	10 1/4	16	61.10	9.44	22.17	0.70	1.44	27.35
12	3.00	7	12 7/8	36.66	4.40	14.37	0.54	1.34	16.01
13	3.00	7 3/4	13	36.66	5.40	14.64	0.55	1.11	14.96
14	3.00	7 5/8	12 1/8	36.66	5.22	12.73	0.54	1.19	16.98
15	3.00	7 1/2	12 1/4	36.66	5.05	13.00	0.54	0.78	17.29
16	5.00	9 3/8	15 5/8	61.10	7.90	21.15	0.69	1.62	29.74
A-1	0.50	0	7 7/8	6.11	0	5.37	0.22	-	0
A-2	0.60	0	8 5/16	7.33	0	5.97	0.23	1.13	0

*1 Weight of impacting bar is 12.22 lb.

*2 Weight of specimen bar is 11.78 lb.

Table 5. Determination of Logarithmic Axial Plastic Strain

Test No.	L_o in.	L_f in.	D_o in.	D_{max} in.	D_{ave} in.	$\frac{D_{ave}}{D_o}$	e_r	$-e_p$
5	0.2454	0.2050	0.1263	0.1395	0.1366	1.0816	0.0784	0.1568
7	0.2503	0.2118	0.1242	0.1370	0.1346	1.0837	0.0804	0.1608
8	0.2531	0.2096	0.1250	0.1376	0.1356	1.0848	0.0815	0.1630
11	0.2722	0.2344	0.1249	0.1371	0.1349	1.0801	0.0770	0.1540
12	0.2562	0.2325	0.1249	0.1322	0.1303	1.0432	0.0423	0.0846
13	0.2515	0.2282	0.1260	0.1335	0.1313	1.0421	0.0412	0.0824
14	0.2514	0.2234	0.1252	0.1322	0.1316	1.0511	0.0498	0.0996
15	0.2509	0.2287	0.1253	0.1330	0.1315	1.0495	0.0483	0.0966
16	0.2510	0.2120	0.1240	0.1373	0.1351	1.0895	0.0857	0.1714
A-1	--	--	--	--	--	--	--	--

Table 6. Stress, Strain, and Strain Rate Determination

Test No.	E_{pw}	$10^{-3}in^3$ vol	$\frac{E_{pw}}{vol}$ $10^{+3}psi$	$-e_p$	Dynamic $-S$	Static $-S_s$	Stress Ratio $\frac{S}{S_s}$	Dynamic $-\dot{e}$	Static $-\dot{e}$	Strain Rate Ratio 10^5
5	25.80	3.07	8.40	0.1568	53,600	46,000	1.16	102.5	$6.25x10^{-4}$	1.64
7	30.46	3.03	10.05	0.1608	62,500	46,000	1.36	116.7	$6.25x10^{-4}$	1.87
8	33.09	3.10	10.67	0.1630	65,300	46,000	1.42	124.6	$6.25x10^{-4}$	1.99
11	27.35	3.33	8.21	0.1540	53,200	46,000	1.16	101.4	$6.25x10^{-4}$	1.61
12	16.01	3.14	5.10	0.0846	60,200	46,000	1.31	71.5	$6.25x10^{-4}$	1.14
13	14.96	3.14	4.77	0.0824	57,800	46,000	1.26	71.6	$6.25x10^{-4}$	1.15
14	16.98	3.10	5.48	0.0996	55,100	46,000	1.20	81.7	$6.25x10^{-4}$	1.31
15	17.29	3.09	5.59	0.0966	57,800	46,000	1.26	81.4	$6.25x10^{-4}$	1.30
16	29.74	3.02	9.85	0.1714	57,400	46,000	1.25	115.8	$6.25x10^{-4}$	1.85
	Average of 5 through 16				58,100		1.26	96.3		1.54

Table 7. Determination of Error in Calculating Dynamic Stress (results for a typical test (#12) analyzed)

Quantity	Value	Possible Error	Error in Terms of Energy, Strain or Volume
h_{iB}	3.00"	±0.005"	±0.06 in-lb
Arc_{iA}	7"	±0.125"	±0.16 in-lb
Arc_{sA}	12 7/8"	±0.0625"	±0.15 in-lb
Arc_{wf}	39.93"	±0.06"	none
Lateral Vibration Amplitude	1.87cm	±0.05cm	±0.07 in-lb
Longitudinal Vibration Amplitude	0.525cm	±0.05cm	±0.005 in-lb
Total Possible Energy Error			±0.44 in-lb
D_{ave}	0.1303"	±0.00005"	±0.0016 in/in
D_o	0.1249"	±0.00005"	
l_o	0.2562"	±0.0001"	± $5x10^{-6}$ in^3

The stress is 60,200psi ± 3,300psi.

Appendix 1

Sample Calculation of Stress, Strain, and Strain Rate

In order to show how the equations summarized on page 34 are used, a sample calculation of stress and strain rate will be made using the data of test number 12 which is a typical test. The experimentally recorded data for test 12 is recorded in the sample data sheet, Fig. 9. The first quantity that must be calculated is the energy available for plastic work

$$E_{pw} = PE_{iB} - PE_{iA} - PE_{sA} - E_{wf} - E_{vib} \tag{48}$$

In order to calculate the energy available for plastic work, the terms on the right hand side of Eq. (48) must be evaluated. They will be evaluated in their order of appearance.

The potential energy of the impacting bar, PE_{iB}, before its release (equal to the total system initial energy) is given by Eq. (8)

$$PE_{iB} = w_{ib}\ (h_{iB}) \tag{8}$$

$$PE_{iB} = 12.22\ (3.00) = 36.66 \text{ in-lb} \tag{59}$$

The potential energy of the impacting bar after the collision, PE_{iA}, is given by Eq. (10)

$$PE_{iA} = w_{ib} (h_{iA}) \tag{10}$$

The height h_{iA} is 0.360 in. using the known arc length of 7" and Eq. (9). The potential energy, PE_{iA}, is then

$$PE_{iA} = 12.22 (0.360) = 4.40 \text{ in-lb} \tag{60}$$

The potential energy of the specimen bar after impact, PE_{sA}, is given by Eq. (11)

$$PE_{sA} = w_{sb} (h_{sA}) \tag{11}$$

where the height, h_{sA}, is found to be 1.22 in. by using Eq. (9) and the known arc length of 12 7/8". The potential energy, PE_{sA}, is then

$$PE_{sA} = 11.78 (1.22) = 14.37 \text{ in-lb} \tag{61}$$

The energy loss due to windage and friction, E_{wf}, is given by Eq. (12)

$$E_{wf} = 0.01342 \text{ (total arc length)} \tag{12}$$

The total arc length is the sum of the arc lengths traveled by both bars before and after impact. The arc length traveled by the impacting bar before impact can be determined from Eq. (9)

$$h = \frac{arc^2}{136} \tag{9}$$

For h = 3.00" the arc length is determined to be 20.20". The total arc length is then

$$\text{total arc length} = Arc_{iB} + Arc_{iA} + Arc_{sA} \tag{62}$$

$$= 20.20 + 7.00 + 12.88 \tag{63}$$

$$= 40.08 \text{ in.} \tag{64}$$

The energy loss due to windage and friction is then

$$E_{wf} = 0.01342\ (40.08) = 0.54 \text{ in-lb} \tag{65}$$

The energy loss due to vibrations is given by Eq (47)

$$E_{vib} = 0.02 + E_{Lat} \tag{47}$$

where E_{Lat} is given by

$$E_{Lat} = 0.375\ (Am_{Lat})^2 \tag{45}$$

The maximum lateral amplitude, Am_{Lat}, is given by Eq. (44)

$$Am_{Lat} = \sqrt{Am_{vert}^{\ 2} + Am_{horiz}^{\ 2}} \tag{44}$$

If $Am_{vert} = 1.30$ cm and $Am_{horiz} = 1.35$cm from Table 3 for test #12 are substituted into (44), the maximum lateral trace amplitude, Am_{Lat}, is

$$Am_{Lat} = 1.87\text{cm} \quad (66)$$

The vibration loss due to lateral vibration is then

$$E_{Lat} = 0.375\ (1.87)^2 = 1.32 \text{ in-lb} \quad (67)$$

The total vibration loss is

$$E_{vib} = 0.02 + 1.32 = 1.34 \text{ in-lb} \quad (68)$$

The energy available for plastic work from (48) is then

$$E_{pw} = 36.66 - 4.40 - 14.37 - 1.34 - 0.54 \quad (69)$$

$$= 16.01 \text{ in-lb} \quad (70)$$

The average flow stress is determined from Eq. (7)

$$S = \frac{E_{pw}}{\text{vol } e_p} \quad (7)$$

In order to determine the stress, S, the volume and logarithmic plastic strain must be calculated. The volume is obtained from the initial dimensions of the specimen tip

$$\text{vol} = \frac{\pi}{4} (0.1249)^2 (0.2562) = 3.14 \times 10^{-3} \text{ in}^3 \tag{71}$$

The logarithmic plastic strain in the axial direction, e_p, is determined from the constant volume condition

$$e_p = -2e_r \tag{50}$$

The logarithmic plastic strain in the radial direction, e_r, is obtained from

$$e_r = \ln \frac{D_{ave}}{D_o} = \ln \frac{0.1303}{0.1249} = 0.0423 \tag{49}$$

The strain e_p is then

$$e_p = -2(0.0423) = -0.0846 \text{ in/in} \tag{72}$$

If the proper substitutions are made, the average flow stress is determined from Eq. (7)

$$S = \frac{16.01}{3.14 \times 10^{-3} (-0.0846)} = -60{,}200\text{psi} \tag{73}$$

The dynamic strain rate found by equating impulse and momentum for the impacting bar is

$$\dot{e} = \frac{e_p \; SA}{m_i \; (\sqrt{2g \; h_{iB}} \; - \sqrt{2g \; h_{iA}})} \qquad (56)$$

Substituting the known values into (56) we find

$$\dot{e} = \frac{-0.0846 \; (63{,}200)(\frac{\pi}{4})(.1303)^2}{\frac{12.22}{386} \left[\sqrt{2(386)(3.00)} \; - \sqrt{2(386)(0.36)} \right]} \qquad (74)$$

$$= -71.5 \text{ in/in-sec} \qquad (75)$$

The dynamic strain rate found from equating impulse and momentum for the specimen bar is

$$\dot{e} = \frac{e_p \; SA}{m_s \; \sqrt{2g \; h_{sA}}} \qquad (58)$$

Substituting known values into (58) we obtain

$$\dot{e} = \frac{-0.0846 \; (63{,}200)(\frac{\pi}{4})(.1303)^2}{\frac{11.78}{386} \; \sqrt{2(386)(1.22)}} \qquad (76)$$

$$= -76.0 \text{ in/in-sec} \qquad (77)$$

Since there is a small difference in the strain rate values obtained [comparing (75) and (77)], the strain rate based on impulse equals momentum for the impacting bar will be used for the rest of the tests.

BIBLIOGRAPHY

Baron, H. G., 1956, Stress-Strain Curves of Some Metals and Alloys at Low Temperatures and High Rates of Strain: Jour. of the Iron and Steel Institute, V. 182, part 4, p. 354-365.

Bell, J. F. and Werner, W. M., 1962, Applicability of Taylor Theory of Polycrystalline Aggregate to Finite Amplitude Wave Propagation in Annealed Copper: Jour. Appl. Physics, V. 33, No.8, p. 2416-2425.

Culver, R. S., 1963, A Study of Dynamic Deformation Phenomenon, Unpublished Doctoral Thesis, Cambridge University.

Davies, E. R. H. and Hunter, S. C., 1960, The Dynamic Compression Testing of Solids by the Methods of the Split Hopkinson Pressure Bar: ARDE Report (MX) 8-60.

Kolsky, H., 1949, An Investigation of the Mechanical Properties of Materials at Very High Rates of Loading: Phys. Soc. (London) Proc., V. B-62, p. 676-700.

Manjoine, M. and Nadai, A., High-Speed Tension Tests at Elevated Temperatures: Am. Soc. Testing Materials, V. 40, p. 822-837.